Four dimensional chaos and intermittency in a mesoscopic model of the electroencephalogram

Mathew P. Dafilis,[1,a)] Federico Frascoli,[2] Peter J. Cadusch,[3] and David T. J. Liley[4,b)]
[1]*Vaccine and Immunisation Research Group, Murdoch Childrens' Research Institute and Melbourne School of Population Health, The University of Melbourne, Carlton VIC 3010, Australia*
[2]*Department of Mathematics and Statistics, The University of Melbourne, Parkville VIC 3052, Australia*
[3]*Faculty of Engineering and Industrial Sciences, Swinburne University of Technology, PO Box 218, Hawthorn VIC 3122, Australia*
[4]*Brain Dynamics Research Unit, Brain and Psychological Sciences Research Centre (BPsyC), Swinburne University of Technology, PO Box 218, Hawthorn VIC 3122, Australia*

(Received 15 November 2012; accepted 22 April 2013; published online 9 May 2013)

The occurrence of so-called four dimensional chaos in dynamical systems represented by coupled, nonlinear, ordinary differential equations is rarely reported in the literature. In this paper, we present evidence that Liley's mesoscopic theory of the electroencephalogram (EEG), which has been used to describe brain activity in a variety of clinically relevant contexts, possesses a chaotic attractor with a Kaplan-Yorke dimension significantly larger than three. This accounts for simple, high order chaos for a physiologically admissible parameter set. Whilst the Lyapunov spectrum of the attractor has only one positive exponent, the contracting dimensions are such that the integer part of the Kaplan-Yorke dimension is three, thus giving rise to four dimensional chaos. A one-parameter bifurcation analysis with respect to the parameter corresponding to extracortical input is conducted, with results indicating that the origin of chaos is due to an inverse period doubling cascade. Hence, in the vicinity of the high order, strange attractor, the model is shown to display intermittent behavior, with random alternations between oscillatory and chaotic regimes. This phenomenon represents a possible dynamical justification of some of the typical features of clinically established EEG traces, which can arise in the case of burst suppression in anesthesia and epileptic encephalopathies in early infancy. [http://dx.doi.org/10.1063/1.4804176]

The occurrence of so-called high order chaotic activity in nonlinear systems has important consequences for the dynamical properties of the phenomenon that a model tries to capture. In fact, the higher the order, the larger is the number of variables needed to correctly describe the irregular and unpredictable dynamics that a system undergoes. Although chaos has been shown to arise out of equations describing the average electrical activity of populations of neurons in the human brain, this is the first time high order chaos has been reported in such a context. Evidence of such high order deterministic dynamics has important implications for the origin of clinically relevant patterns in electroencephalography and for the effective use of signal processing techniques in theoretical and applied neuroscience.

I. INTRODUCTION

There exist very few examples in the literature of dynamical systems described by sets of coupled nonlinear ordinary differential equations (ODEs), which exhibit simple chaotic attractors of dimension $3+\epsilon$, where ϵ is a positive number smaller than one. The occurrence of such dynamics is often referred to as "four dimensional chaos," as there needs to be at least four degrees of freedom to generate such behaviour. An early example of such chaos was presented by Lorenz,[1] in a system of polynomial-like, coupled ODEs. Sigeti[2] reported an accurate calculation of the Lyapunov exponents for the Lorenz 4D model, and showed that the Kaplan-Yorke dimension (D_{KY}) is 3.34. Some other notable examples of four dimensional chaos include those by Hudson, Rössler, and Killory,[3] where for a piecewise-linear set of ODEs, the authors computed the Lyapunov spectrum and subsequently calculated a D_{KY} of 3.035. Similar high dimensional chaotic activity was also found in a model of fluid flow,[4] with a dimension for the attractor of 3.04. It is important to distinguish between four dimensional chaos, with a dimension of $3+\epsilon$, and "hyperchaos." Although in the latter the dimension is also at least $3+\epsilon$, the former only possesses a single positive Lyapunov exponent, whereas hyperchaos is instead associated with two or more positive exponents.[5]

In this paper, a clear example of a chaotic attractor whose D_{KY} is significantly above three is given, with one, unique, largest Lyapunov exponent, which is strongly positive. These findings are born out of a parameter space search of Liley's mesoscopic theory of the electroencephalogram (EEG).[6] Interestingly, the chaotic set discussed in this work exhibits parameter values that are essentially within the physiologically admissible range. The full

[a)]Electronic mail: mdafilis@unimelb.edu.au; previously at Brain Dynamics Research Unit, Brain and Psychological Sciences Research Centre (BPsyC), Swinburne University of Technology, PO Box 218, Hawthorn VIC 3122, Australia.
[b)]Electronic mail: dliley@swin.edu.au

Lyapunov spectrum, relevant time series and power spectra, and a phase plot section of the dynamics are discussed in the light of previously reported results for Liley's model. The origin of this high dimensional attractor is then established, using a one-parameter bifurcation analysis, showing that the system supports an inverse period doubling cascade. Its presence is also responsible for so-called type III intermittent behavior,[7] with a characteristic hopping regime between oscillatory and chaotic dynamics. The similarity between this kind of dynamics and typical EEG traces arising in pathological and sedated brain states is examined. We finally conclude our investigation with a discussion about the meaning of the existence of such four dimensional chaos for the analysis of real-world EEG signals.

II. LILEY'S THEORY OF THE EEG

Liley's theory of the EEG is a complete spatiotemporal theory of the dynamics of the mammalian electroencephalogram. Here, only a brief description of its constitutive ODEs is presented, which represent a mesoscopic, spatially homogeneous reduction of the general formulation. This model is inspired by previous work by Freeman and collaborators, who have extensively investigated the role of dynamical systems and chaos in theories of brain dynamics.[8–10] Further details, including a comprehensive physiological justification for the model's equations, can be found in Liley, Cadusch, and Dafilis.[6] The following reduced approach has proven to be a fruitful generator of significant nonlinear behavior, such as generalised multistability in the initial-condition space,[11] robust chaos in parameter space with fat fractal scaling,[12] and a Shilnikov's saddle-node bifurcation route to chaos.[13] The latter is of particular interest as Liley's theory represents one of the few examples of a real world mathematical model that exhibits such a rare bifurcation scenario. Finally, these ODEs have also found important applications in the characterisation of some features of epileptic activity[14] and in the study of anaesthesia.[15,16]

The spatially homogeneous formulation of Liley's model is represented by the following equations:

$$\tau_e \frac{dh_e}{dt} = (h_{er} - h_e) + \frac{h_{eeq} - h_e}{|h_{eeq} - h_{er}|} I_{ee} + \frac{h_{ieq} - h_e}{|h_{ieq} - h_{er}|} I_{ie}, \quad (1)$$

$$\tau_i \frac{dh_i}{dt} = (h_{ir} - h_i) + \frac{h_{eeq} - h_i}{|h_{eeq} - h_{ir}|} I_{ei} + \frac{h_{ieq} - h_i}{|h_{ieq} - h_{ir}|} I_{ii}, \quad (2)$$

$$\frac{d^2 I_{ee}}{dt^2} + 2a \frac{dI_{ee}}{dt} + a^2 I_{ee} = Aae\{N_{ee} S_e(h_e) + p_{ee}\}, \quad (3)$$

$$\frac{d^2 I_{ie}}{dt^2} + 2b \frac{dI_{ie}}{dt} + b^2 I_{ie} = Bbe\{N_{ie} S_i(h_i) + p_{ie}\}, \quad (4)$$

$$\frac{d^2 I_{ei}}{dt^2} + 2a \frac{dI_{ei}}{dt} + a^2 I_{ei} = Aae\{N_{ei} S_e(h_e) + p_{ei}\}, \quad (5)$$

$$\frac{d^2 I_{ii}}{dt^2} + 2b \frac{dI_{ii}}{dt} + b^2 I_{ii} = Bbe\{N_{ii} S_i(h_i) + p_{ii}\}, \quad (6)$$

where

$$S_q(h_q) = S_q^{\max}/(1 + \exp(\sqrt{2}(h_q - \theta_q)/s_q), \qquad q = e, i.$$

The main state variables of the model are h_e and h_i, representing the mean modelled membrane potentials of the excitatory and inhibitory cortical neural populations, respectively. The variable h_e, on the basis of physiological argument, is assumed to model the EEG recorded from the brain.[6] The I terms describe synaptic dynamics: in short, they express the synaptic drive to the modelled neural populations, due to feedback between neurons and input from external sources. The model also incorporates the effects of the resting (h_{er} and h_{ir}) and reversal potentials (h_{eeq} and h_{ieq}), population time constants are given by τ_e and τ_i, and synaptic weights are expressed by A and B, with synaptic rate constants a and b. The N_{jk} describe the density of synapses from population j to population k, p_{jk} is the external pulse densities of type j to population k, mainly capturing the effect of the input coming from the thalamus on the cortex. Variations of p_{ee}, namely the excitatory input to the excitatory neuronal population, are particularly relevant for the generation of complex behavior. As such p_{ee} is the parameter selected to be studied via bifurcation analysis. Sigmoidal parameters include θ_q, the threshold for the neural population, s_q, which is proportional to the standard deviation of the firing threshold distribution of the neural population, and $S_q^{\max}$, which includes the effects of the refractory period and describes the maximum activity of the neuron population at any one instance.

III. METHODS

A. Model parameters

The parameters for the model which generated these dynamics are $p_{ee} = 24.523$ pulses per millisecond (or ms^{-1}), $p_{ei} = 2.299\,\text{ms}^{-1}$, $p_{ie} = p_{ii} = 0$, $A = 0.24\,\text{mV}$, $B = 3.76\,\text{mV}$, $1/a = 24.89$ ms, $1/b = 6.59$ ms, $h_{er} = h_{ir} = -70\,\text{mV}$, $h_{eeq} = 45\,\text{mV}$, $h_{ieq} = -90\,\text{mV}$, $\tau_e = 66$ ms, $\tau_i = 24$ ms, $S_e^{\max} = 0.5$, $S_i^{\max} = 0.5$, $N_{ee} = 3034$, $N_{ei} = 3500$, $N_{ie} = N_{ii} = 536$, $\theta_e = -41\,\text{mV}$, $\theta_i = -49\,\text{mV}$, $s_e = 1\,\text{mV}^{-1}$, and $s_i = 1.5\ \text{mV}^{-1}$. Further details on the parameterisation of the model can be found in Liley, Cadusch, and Dafilis.[6] Note that all parameters are essentially within physiologically admissible intervals. However, p_{ee} extends outside a physiologically "normal" range of $0 < p_{ee} < 10\,\text{ms}^{-1}$, and thus might correspond to a pathological or some other abnormal state.

B. Time-series and power spectrum

All model time series were obtained using XPPAUT,[17] by numerically integrating Eqs. (1)–(6) using a time step of 1 ms for a total duration of 105 s. In order to retain a strong connection to the modelled physiology, equations were not de-dimensionalised, such that physiologically appropriate units were retained throughout. The first 5 s were discarded (transient), leaving a time series of 100 s (i.e., 100 000 points). Representative 1000 ms long time series for h_e and h_i are shown in parts (a) and (b) of Fig. 1. Subsequent power spectral analysis was performed on the full 100 s time series using MATLAB, yielding a frequency resolution of 0.01 Hz

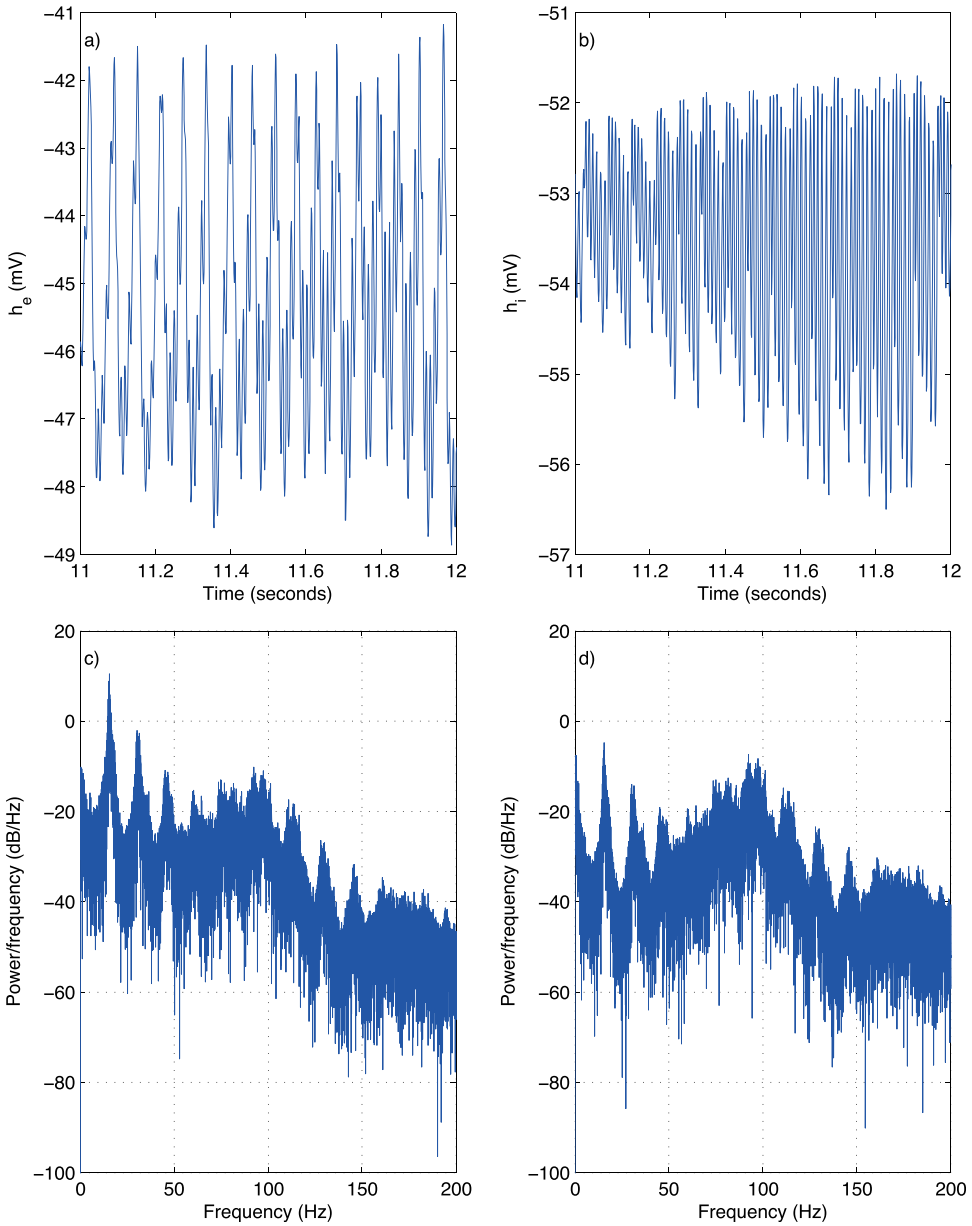

FIG. 1. Time series ((a) and (b)) and spectra ((c) and (d)) for h_e and h_i for the parameter set under investigation. The broadband nature of the power spectrum is evident in panels (c) and (d), which are clearly indicative of chaotic dynamics. Note the presence of dominant rhythms and higher harmonics alongside the broadband power spectral activity, as well as the significant amount of power at high frequencies, especially in the band 80–100 Hz.

and a Nyquist frequency of 500 Hz. Parts (c) and (d) of Fig. 1 show the spectra for h_e and h_i.

C. Lyapunov spectrum

Custom written code was used to calculate the full Lyapunov spectrum of the system, using an implementation of the Christiansen-Rugh algorithm[18] to compute a continuous Gram-Schmidt orthonormalization. The resulting algorithm works by augmenting the given set of ODEs with additional terms that capture the Lyapunov exponents of the system: the original 10 dimensional system is augmented such that 120 coupled, nonlinear, first order ODEs need to be solved. This resulting system of 120 nonlinear ODEs was integrated using the adaptive, stiff solver CVODE,[19] with the method of backward differentiation. Efficiency and accuracy of the solutions were improved by supplying a symbolically determined Jacobian matrix, together with the use of the dense linear solver option. In order to calculate the spectrum of Lyapunov exponents, the system of 120 nonlinear ODEs was integrated over 100 s of simulated time. For this integration convergence was established. Interestingly, although different parameter values are involved in the present example, previous numerical experiments have indicated that this choice of simulated time provides reasonable convergence.[12] This was then repeated over 25 independent simulation runs, each with different random initial conditions. The mean and standard deviation of each Lyapunov exponent of the spectrum was then calculated.

D. Kaplan-Yorke dimension

The Lyapunov spectrum was used to determine $D_{KY,}$ via an appropriate reduction of the more general formulation.[5] Specifically, for the chaotic attractor presented in this paper, if $\lambda_i\,(i = 1, \ldots, 10,\ \lambda_1 \geq \lambda_2 \ldots)$ represents the ith exponent in the spectrum, it is found that $|\lambda_1| > |\lambda_3|$ and $\lambda_1 + \lambda_2 + \lambda_3 > 0$, whereas $\lambda_1 + \lambda_2 + \lambda_3 + \lambda_4 < 0$. On this basis, D_{KY} is given by

$$D_{KY} = 3 - \frac{\lambda_1 + \lambda_2 + \lambda_3}{\lambda_4}. \quad (7)$$

E. One-parameter bifurcation analysis

Bifurcation diagrams were obtained using the software AUTO,[20] a well-established program for continuation in dynamical systems. Analysis proceeded with respect to p_{ee} as the principle bifurcation parameter, for the reasons that (i) p_{ee} represents a physiologically meaningful control parameter, and (ii) p_{ee} has been meaningfully used to identify the emergence of chaos and a range of other dynamical behaviours in this model.[11,13]

IV. RESULTS AND DISCUSSION

In order to determine the existence of a chaotic attractor, visual inspection of time-series and power spectra is generally helpful, although not always decisive. The four panels of Fig. 1 all illustrate different aspects of the dynamics of interest in this study. Part (a) of the figure shows a sample of the time series for h_e, whereas part (b) shows the corresponding time series for h_i, the mean soma membrane potential of the inhibitory neuronal population. The irregular appearance of these time series, given their aperiodic nature, strongly suggests the existence of chaos for the parameter values reported in the figure caption. The power spectrum, Fig. 1(c), confirms such aperiodicity by being characterized by a broadband distribution of power that additionally reveals spectral peaks corresponding to electroencephalographically plausible alpha (8–13 Hz), beta (13–30 Hz), and gamma (>30 Hz) band activity. At the same parameter values, a two dimensional, discrete phase plot (with $h_e(\Delta t)$ on the abscissa and $h_i(\Delta t)$ on the ordinate) is shown in Fig. 2, with $\Delta t = 1$ ms. The largely amorphous structure of this cross section through the attractor confirms that its dimension is of at least three, since attractors of lower dimensionality would have a simpler, sharper and more "focused" appearance.

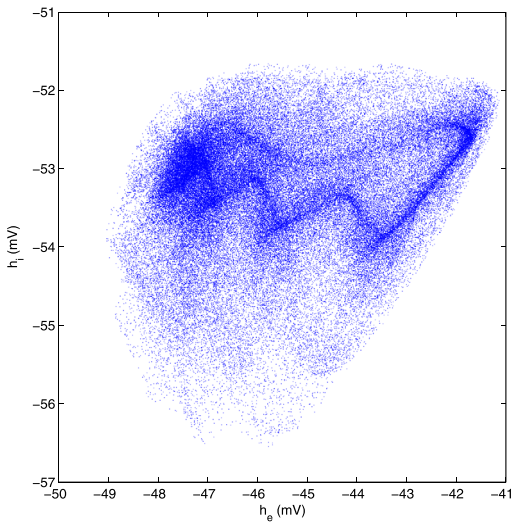

FIG. 2. Phase plot for $h_e(\Delta t)$ and $h_i(\Delta t)$ for the parameter set under investigation, with $\Delta t = 1$ ms. The shape is peculiarly blurred, with a persistent shadow of points originating from the supporting orbit around which the chaotic activity develops.

Table I shows the estimated Lyapunov spectrum. The strong λ_1 with a value of 9.6 (base e) per second clearly confirms the presence of chaotic dynamics. This and $\lambda_2 = 0$ indicate that "simple" and not "hyper" chaos has been found. Applying Eq. (7) to the exponents results in a D_{KY} of 3.28 (N = 25, SD 0.02). Note that this formula is used with the original 25 Lyapunov spectra to determine the statistics, as opposed to calculating D_{KY} for the averaged Lyapunov exponents. The value of D_{KY} is in line with examples of four dimensional chaos present in the literature and previously cited.[2–4]

It is now useful to investigate the origin of this phenomenon with the help of bifurcation analysis, and continue a stable equilibrium solution in the parameter p_{ee} over the range encompassing the value of p_{ee} used to generate the aperiodic activity of Fig. 1. The bifurcation diagrams contains three Hopf bifurcation HB1, HB2, and HB3 for values $p_{ee} = 4.86$, 29.49, and 29.76 ms^{-1}, where only the last two are shown in Fig. 3(a). From these bifurcations, a complex scenario of stable and unstable periodic orbits unfolds. The section of the plot relevant to the generation of high dimensional chaos is shown in Fig. 3(b), where HB2 and HB3 appear in the bottom right corner, indicated by open triangles. A stable orbit (in orange) emerges from HB3, loses its stability around $p_{ee} = 29\,\text{ms}^{-1}$ via a torus (TR) bifurcation and continues for decreasing values of the parameter without influencing the area of the diagram where the high dimensional chaotic attractor exists. An unstable orbit (in green) instead originates from HB2 and gives rise to a number of complex bifurcations including period doubling (PD), saddle-nodes on periodic orbits (SNLC), and tori. In the top part of Fig. 3(a), two inverse period-doubling cascades are present, starting respectively at $p_{ee} = 25.16\,\text{ms}^{-1}$ and $p_{ee} = 26.05\,\text{ms}^{-1}$. A blow-up of this area is shown in Fig. 3(b), where the interplay among the diverse orbits can be better appreciated.

The stable branches of each cascade are shown by continuous black lines. The transitions between accumulation of PD points and the genesis of chaos occur at about

TABLE I. Lyapunov spectrum for the dynamics under investigation for the Liley model. The mean and standard deviation of each Lyapunov exponent was obtained from 25 independent simulation runs each started from different, random, initial conditions. For further details refer to the Methods section.

λ	Mean	SD
λ_1	9.6	0.6
λ_2	0.00	0.02
λ_3	−6.4	0.5
λ_4	−11.5	0.6
λ_5	−40.12	0.01
λ_6	−40.32	0.01
λ_7	−151.65	0.01
λ_8	−151.86	0.01
λ_9	−480.5	0.9
λ_{10}	−1447	4

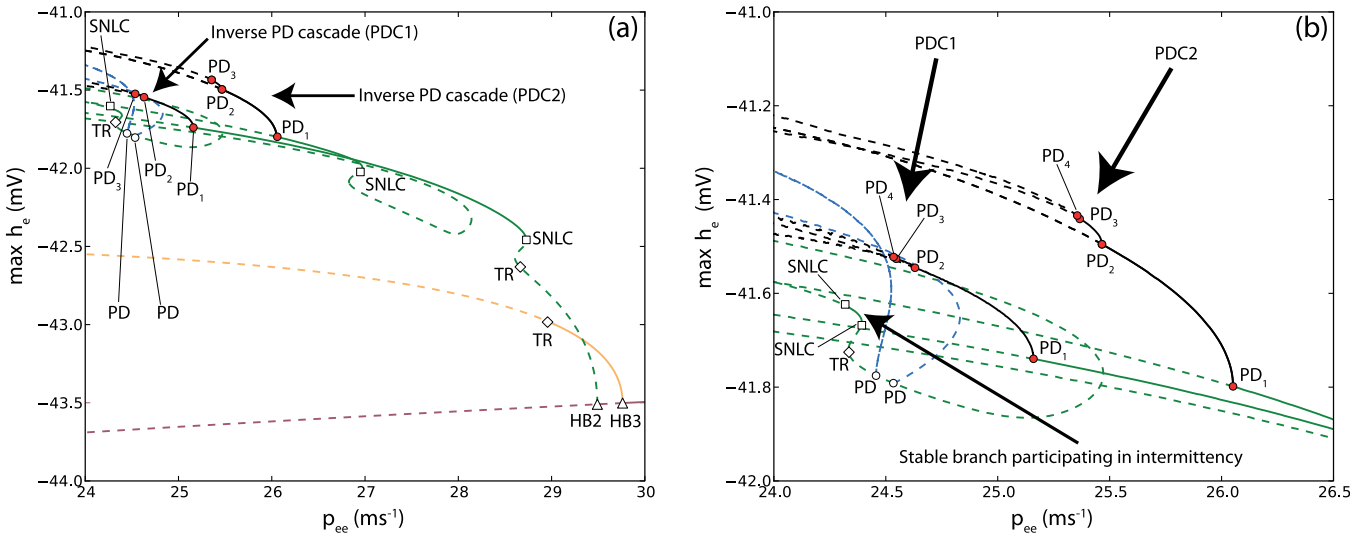

FIG. 3. Relevant section of the one parameter bifurcation plot in p_{ee}. In (a), two Hopf points (triangles) are present in the bottom right corner of the figure, from which orbits with different properties emerge. Different colors indicate different branches, stable (unstable) branches are continuous (dashed), whereas orbit bifurcations are indicated by circles (period doubling, PD), squares (saddle-nodes on limit cycle, SNLC), and diamonds (torus, TR). Both period doubling cascades are in black, PD points are in red, and generations (up to three) are indicated by subscripts. The ordinate is given by the maxima of h_e, hence only the top halves of the familiar pitchfork shapes of period doubling cascades is presented. The first, second, and third generations of these cascades are displayed. In (b), a closer detailed depiction of the two inverse period doubling cascades is provided. The stable attractor that participates in the intermittency phenomenon described in this paper belongs to the stable branch in green in the interval $24.35\,\mathrm{ms}^{-1} < p_{ee} < 24.39\,\mathrm{ms}^{-1}$ and $-41.63\,\mathrm{mV} < h_e < -41.66\,\mathrm{mV}$, between the two SNLC points.

$p_{ee} = 24.53\,\mathrm{ms}^{-1}$ for PDC1 and $p_{ee} = 25.35\,\mathrm{ms}^{-1}$ for PDC2. The first of these regions is close to the value of $p_{ee} = 24.523\,\mathrm{ms}^{-1}$, at which the chaotic time series depicted in Fig. 1 is found. It is evident that PDC1 is responsible for the high dimensional chaos observed in the model. If a comparison is made between the chaotic time series and the orbits belonging to the stable branch in a late generation of the cascade PDC1 shown in Figs. 4(a) and 4(b), these last orbits behave as supports for the chaotic time series. The second inverse cascade PDC2 is itself leading to a different chaotic attractor and is one of the many examples of similar period doubling cascades the model exhibits for the present and for other parameter sets.

At this point, two observations are relevant. First, each of the inverse PD cascades is matched by a symmetric, direct PD cascade occurring for orbits at lower values of the simulated extracortical (thalamic) input p_{ee}, beginning at values $p_{ee} = 4.90\,\mathrm{ms}^{-1}$ and $p_{ee} = 4.92\,\mathrm{ms}^{-1}$ for cases 1

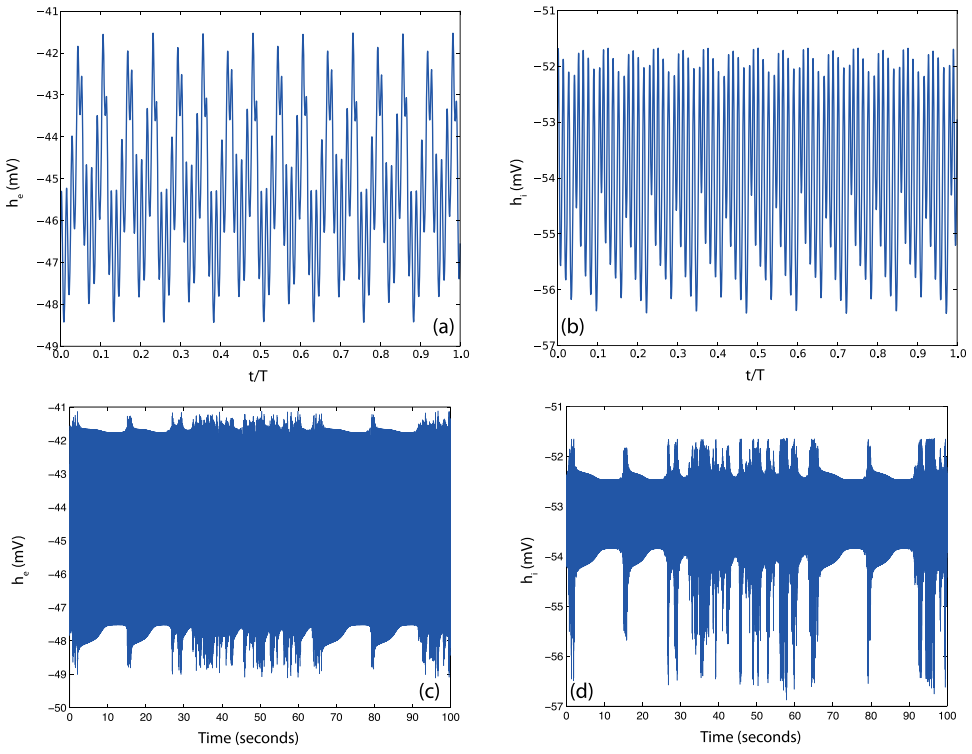

FIG. 4. In (a) and (b), the stable orbits from the fourth generation branch in the period doubling cascade PDC1 are shown, for $h_e(t)$ and $h_i(t)$. Orbits are scaled so that the intrinsic period of the oscillation is $T = 1$. Notice the similarity with part of the chaotic time series in Fig. 1. In (c) and (d), examples of intermittency between the chaotic attractor and the stable orbit, for $p_{ee} = 24.4\,\mathrm{ms}^{-1}$ are illustrated. The intervals of small amplitude oscillations correspond to the system being on the stable attractor, and large amplitude bursts are due to the chaotic attractor.

and 2, respectively (not shown). This means that branches of the direct and inverse PDC1 and PDC2 are the same: orbits originating at PD_1 around $p_{ee} = 25.3\,\mathrm{ms}^{-1}$ in the inverse PDC1 terminate at the first generation PD in the direct cascade around $p_{ee} = 4.90\,\mathrm{ms}^{-1}$, the branch starting at PD_2 in the inverse PDC1 around $p_{ee} = 24.6\,\mathrm{ms}^{-1}$ ends at the second generation PD in the direct PDC, and so on. Second, the existence of inverse cascades implies the presence of intermittency, a sample of which is shown in Figs. 4(c) and 4(d). This phenomenon is readily apparent for values of p_{ee} approximately between the accumulation of PD points from PDC1 and the small stable branch below this cascade, starting at $p_{ee} = 24.39\,\mathrm{ms}^{-1}$ and shown in Fig. 3(b). Depending on the initial condition for the system variables and the vicinity of p_{ee} either to PDC1 or the stable branch, the system bounces between the chaotic and the stable attractors without permanently settling on any of the two.[21] This behavior, in association with inverse PDCs, has been labelled type III intermittency, as opposed to types I and II, which are linked to different bifurcation scenarios.[7] Although Liley's neural field equations are known to support multistability,[11] this is the first time that intermittency has been reported.

V. CONCLUSIONS

The results presented in this work are indicative of four-dimensional chaos within Liley's model, and the Lyapunov spectrum clearly suggests an integer part of three for the D_{KY} with a significant fractional part. The structure of the attractor, whilst technically of a low dimension if compared to other models in the literature that show a $D_{KY} \gg 3$, has rather an amorphous appearance in cross section (see Fig. 2). This is very relevant, since, at first examination, it may not be possible to discern the attractor from noise either with a simple visual inspection or even with nonlinear time-series analysis techniques.[22]

The dynamics at this modelled scale in fact approximates those found at the scale of the macrocolumn, a microscopic aggregate of approximately 10^5 neurones. There are tens of thousands of such macrocolumns when one considers the scale of the entire brain, each massively interconnected to each other via the intracortical and cortico-cortical fibres. Let us assume that an individual macrocolumn could indeed present a relatively amorphous attractor as the one presented in this work. Since one EEG electrode records the aggregate activity of many hundreds of them, and since noise is always present in the brain at all spatial and temporal scales, nonlinear time series analysis methods could fail to recognise the appropriate dynamics, mistaking it for noise. The real signal could indeed be a combination of chaos and noise, but its nonlinear deterministic structure could not be ascertained with existing signal processing methods. In a recent work, the authors have highlighted some of the problems associated with those methods when applied to simple, nonlinear dynamical systems.[23] In the light of this and of the findings discussed in the current work, the characterisation of the nature of EEG dynamics in real contexts still presents major theoretical and practical challenges.[24] Further investigations are underway in order to determine the extent of high dimensional chaos in parameter space, and understand the local and global mechanisms, which give rise to such phenomena.

The occurrence of an inverse period doubling cascade in Liley's reduced equations is a novel finding. This cascade is associated with type III intermittency, which has never been reported for this system. This is not surprising in a model, which has been known to be a source of complexity, chaos and emergent behavior. It should be noted that this phenomenon has interesting connections with experimentally established EEG patterns, showing suppression of bursts, capturing some of their distinctive features. Typical traces of such kind are characterised by persistent isoelectric epochs, which are irregularly interrupted by spiky activity.[25] The hopping nature of intermittency in Fig. 4 is dominated by the alternation of short-time, large-amplitude chaotic "bursts" with long-time, small-amplitude oscillatory periods, which give rise to patterns close to the ones observed in clinical settings. These types of EEG signals have been encountered in a variety of clinical contexts, in particular in anesthesia[26] and epileptic encephalopathies occurring in early infancy.[27]

ACKNOWLEDGMENTS

Writing this, M.P.D., F.F., and D.L. have been supported by ARC grant DP0879137, entitled "Neurobiological computation using self organization."

[1]E. N. Lorenz, "The local structure of a chaotic attractor in four dimensions," Physica D **13**, 90–104 (1984).
[2]D. E. Sigeti, "Exponential decay of power spectra at high frequency and positive Lyapunov exponents," Physica D **82**, 136–153 (1995).
[3]J. L. Hudson, O. E. Rössler, and H. C. Killory, "Chaos in a four-variable piecewise-linear system of differential equations," IEEE Trans. Circuits Syst. **35**, 902–908 (1988).
[4]E. Abu-Ramadan, J. M. Hay, and R. E. Khayat, "Characterization of chaotic thermal convection of viscoelastic fluids," J. Non-Newtonian Fluid Mech. **115**, 79–113 (2003).
[5]J. C. Sprott, *Chaos and Time-Series Analysis* (Oxford University Press, Oxford, 2003).
[6]D. T. J. Liley, P. J. Cadusch, and M. P. Dafilis, "A spatially continuous mean field theory of electrocortical activity," Network: Computation in Neural Systems **13**, 67–113 (2002).
[7]Y. Pomeau and P. Manneville, "Intermittent transition to turbulence in dissipative dynamical systems," Commun. Math. Phys. **74**, 189–197 (1980).
[8]R. Ilin and R. Kozma, "Stability of coupled excitatory-inhibitory neural populations and application to control of multi-stable systems," Phys. Lett. A **360**, 66–83 (2006).
[9]W. J. Freeman, "Tutorial in neurobiology: From single neurons to brain chaos," Int. J. Bifurcation Chaos **2**, 451–482 (1992).
[10]W. J. Freeman and S. Jakubith, "Bifurcation analysis of continuous time dynamics of oscillatory neural networks," in *Brain Theory*, edited by A. Aertsen (Elsevier Science Publishers B.V., Netherlands, 1993).
[11]M. P. Dafilis, F. Frascoli, P. J. Cadusch, and D. T. J. Liley, "Chaos and generalised multistability in a mesoscopic model of the electroencephalogram," Physica D **238**, 1056–1060 (2009).
[12]M. P. Dafilis, D. T. J. Liley, and P. J. Cadusch, "Robust chaos in a model of the electroencephalogram: Implications for brain dynamics," Chaos **11**, 474–478 (2001).
[13]L. van Veen and D. T. J. Liley, "Chaos via Shilnikov's saddle-node bifurcation in a theory of the electroencephalogram," Phys. Rev. Lett. **97**, 208101 (2006).

[14]D. T. J. Liley and I. Bojak, "Understanding the transition to seizure by modeling the epileptiform activity of general anesthetic agents," J. Clin. Neurophysiol. **22**, 300–313 (2005).
[15]I. Bojak and D. T. J. Liley, "Modeling the effects of anesthesia on the electroencephalogram," Phys. Rev. E **71**, 041902 (2005).
[16]F. Frascoli, L. Van Veen, I. Bojak, and D. T. J. Liley, "Metabifurcation analysis of a mean field model of the cortex," Physica D **240**, 949–962 (2011).
[17]B. Ermentrout, *Simulating, Analyzing, and Animating Dynamical Systems: A Guide to* XPPAUT *for Researchers and Students* (SIAM, Philadelpha, PA, 2002).
[18]F. Christiansen and H. H. Rugh, "Computing Lyapunov spectra with continuous Gram-Schmidt orthonormalization," Nonlinearity **10**, 1063–1072 (1997).
[19]S. D. Cohen and A. C. Hindmarsh, "CVODE, a stiff/nonstiff ODE solver in C," Comput. Phys. **10**, 138–143 (1996).
[20]E. J. Doedel, "AUTO: A program for the automatic bifurcation analysis of autonomous systems," Congr. Numer. **30**, 265–284 (1981).
[21]E. Ott, *Chaos in Dynamical Systems* (Cambridge University Press, New York, NY, 2002).
[22]H. Kantz and T. Schreiber, *Nonlinear Time Series Analysis* (Cambridge University Press, New York, NY, 2004).
[23]M. P. Dafilis, N. C. Sinclair, P. J. Cadusch, and D. T. J. Liley, "Re-evaluating the performance of the nonlinear prediction error for the detection of deterministic dynamics," Physica D **240**, 695–700 (2011).
[24]C. J. Stam, "Nonlinear dynamical analysis of EEG and MEG: Review of an emerging field," Clin. Neurophys. **116**, 2266–2301 (2005).
[25]M. Steriade, F. Amzica, and D. Contreras, "Cortical and thalamic cellular correlates of electroencephalographic burst-suppression," Electroencephalogr. Clin. Neurophysiol. **90**, 1–16 (1994).
[26]W. P. Akrawi, J. C. Drummond, C. J. Kalkman, and P. M. Patel, "A comparison of the electrophysiologic characteristics of EEG burst-suppression as produced by isoflurane, thiopental, etomidate, and propofol," J. Neurosurg. Anesthesiol. **8**, 40–46 (1996).
[27]S. Ohtahara and Y. Yamatogi, "Epileptic encephalopathies in early infancy with suppression-burst," J. Neuroclin. Neurophys. **20**, 398–407 (2003).